Advances in Colloid and Interface Science, 34 (1991) 135–173
Elsevier Science Publishers B.V., Amsterdam

Characterization of UF Membranes

Membrane Characteristics and Characterization Techniques

F. P. Cuperus* and C. A. Smolders
University of Twente, Department of Chemical Technology
Center for Membrane Science and Technology
P.O. Box 217, 7500 AE Enschede, The Netherlands

1 Introduction

The field of membrane filtration is currently enjoying a great deal of interest and its field of application is expanding rapidly. Since membrane separations are possible at moderate process conditions the application of membrane filtration in food industry and biotechnology is growing very fast [1]. Furthermore, the possibility to perform separations at low energy costs makes membrane filtration competitive with classical separation techniques. Although the performances of the current membrane systems are sometimes quite satisfying, the fundamentals of membrane separation actions, irrespective whether it concerns gas separation or microfiltration membranes, are not very well understood yet. One of the reasons for this apparent contradiction is that the physical and chemical nature of the applied membranes is intricate, whereas the relation between the membrane structure and the actual performance, i.e., the transport mechanism, is very complex [1-3]. It is recognized nowadays that these problems can only be overcome when the relevant data, describing the membrane structure and transport properties, are known accurately. These parameters can only be found when different characterization techniques are combined. In this paper a number of techniques which are used for the characterization of porous membranes are reviewed. Although the present survey is not entirely complete, it certainly covers the techniques which are sufficiently developed to be exploited with some success [3].

* *Present Affiliation: ATO Agrotechnological Research Institute, P.O. Box 17, 6700 AA Wageningen, The Netherlands.*

0001-8686/91/$13.65

2 Characterization and Membrane History

Filtration processses were already known and described in the ancient Chinese and Egyptian cultures, still it took a very long time before researchers started to investigate the fundamentals of the 'new' phenomena of preferential transport through semi-permeable barriers, i.e., before membrane filtration turned into membrane science. For instance, La Hire (1640-1718) discovered that, compared to ethanol, water diffused preferentially through a porc bladder. Nollet and Dutrochet (about 1750) used membranes in their osmotic pressure experiments, whereas Graham (1805-1869) used membranes for the separation of crystals from colloids (1854) and accomplished the enrichment of oxygen from air (1863). At the same time, Traube produced the first artificial membranes and many other researchers used membranes in their experiments (Fick, Raoult, van 't Hoff). They also developed the first fundamental theories about membrane structures and transport mechanisms. Graham noted the importance of solubility of components in membranes and, in 1855, Lhermite showed that in principle two different membrane types do exist: porous and non-porous ones. Lhermite was also the first who stated the 'solution theory', i.e., permeation as the result of specific interactions between the membrane material and the permeant, but he also recognized that this theory and the 'capillary theories' merge gradually into one another. When Bechhold [4], in 1907, found that the porosity of nitrocellose membranes could be influenced by the manipulation of the collodion concentration in the casting solution, more possibilities became available to study the characteristics of porous membranes thoroughly. Bechhold also developed a technique to evaluate pore sizes in membranes, which is presently known as the 'bubble pressure method'. Between 1924 and 1926, Zsigmondi systematically investigated porous filter media, which eventually led to the first commercially produced membranes by the Sartorius company [5].

During World War II the development and use of membranes became more important. In Germany, where many cities were being destroyed in air-raids, Sartorius membranes were used in the bacteriological examination of water quality. In the US, the USSR, Great Britain and France, ceramic porous membranes were developed for the enrichment of the gaseous uranium hexafluoride U^{235} isotope. Because the separation efficiency of such membranes for the isotope is very poor, millions of square meters of membrane area had to be used.

After the war US-reseachers adopted the knowledge of Sartorius and developed new, better membranes. These polymeric membranes were all of the porous type with pore sizes of at least a few tenths of a micron. Except for the application in isotope enrichment and artificial kidneys, membranes were used only on a small scale for academic and medical purposes. Membranes with different pore sizes or even dense membranes could be made, but showed too poor performance in terms of permeability to be interesting for industrial applications. Only after the development of the anisotropic membrane by Loeb and Sourirajan in 1960, these problems were successfully attacked and a range of new applications became possible. Anisotropic membranes consist of a

thin skin layer, which is the essential effective separation layer and a porous sublayer providing them with the required mechanical stability (figure 1). By means of the so-called phase inversion process it became possible to synthesize a variety of porous and non-porous anisotropic membranes from a wide range of polymers. Since then membrane processes like reverse osmosis (RO), ultrafiltration (UF) and microfiltration (MF) and later gas separation were developed for applications on an industrial scale.

Figure 1. Schematic representation of an isotropic (A) and an anisotropic (B) membrane structure.

As more complicated membrane systems are developed, the need for consistent theories on membrane structure and membrane performance becomes urgent. A better understanding of the separation mechanism can lead to improved membranes or membrane processes but requires the development of characterization methods and the improvement of models and theories.

3 Characterization: Some Definitions Concerning Porous Membranes

Characterization, as applied to membrane systems, can have different meanings depending on the purpose for which the acquired data are needed. It may be desirable to have fundamental information about physical properties such as porosity, pore size and pore size distribution but, on the other hand, information concerning the performance of a membrane may be more important. For instance: when the best membrane for a certain separation must be chosen or when the quality of membranes in the manufacturing processes must be controlled. This demands the understanding of the performance properties of the membrane in close relation to the characteristic data for the membrane structure. In addition, the membrane process should be considered with respect to the process streams and the technological features of the whole system [6].

From these considerations, we can define two categories of characteristic parameters: *'performance related parameters'* and *'morphology related parameters'*. The development of consistent theories on membrane structure and performance needs the linkage between the performance and morphology related parameters by a model (figure 2) [7]. For real systems such models may be very complicated. This is not only due to the intricate membrane structures, but also to the complexity of the transport mechanisms and the presence of interfering phenomena

like concentration polarization and fouling. The interplay of all these phenomena is responsible for the ultimate membrane performance. From the foregoing recapitulation, it should be clear that characterization involves the development of three main areas:

- accurate determination of the porous structure;
- insight in phenomena which occur during filtration;
- development of models to interpret relationships between preparation, morphology and properties of membranes.

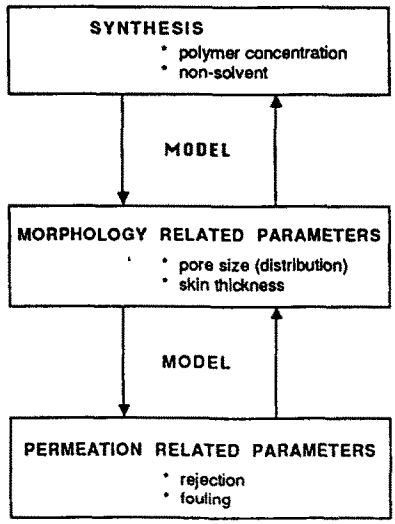

Figure 2. Links between membrane synthesis, morphology related parameters and permeation related parameters.

In literature several characteristic parameters for membrane performance are enumerated. Permeability, rejection, (effective) diffusion coefficients and separation factors are considered to be the most important ones. Morphology related parameters are pore size, pore size distribution, membrane thickness (for anisotropic membranes: skin thickness), pore shape and various chemical and physical properties like adsorptive and absorptive properties and charge density.
The definition of important membrane characteristics is often a problem, which is not only due to a vague description of such parameters but also is a matter of terminology. For that reason the European Society for Membrane Science and Technology (ESMST) published a list of recommended terms to be used in texts and discussions on membranes [8]. Porous materials have been investigated fundamentally since 1777 (Fontana and Scheel) and consequently the terminology to describe the porous structures has been developed since then. In the following chapters we focus on porous ultrafiltration membranes and therefore some of these established terms are discussed here.

Ever since the first estimation of pore size in charcoal by Mitscherlich in 1843 [9], the pore size concept has been the most widely used characteristic of porous materials. Dubinin proposed the definition of three pore size classes according to the average width of the pores (which is of course also a little bit arbitrary):

a. macropores: widths exceeding 50 nm (0.05 μm);
b. mesopores: widths between 50 and 2 nm;
c. micropores: widths not exceeding 2 nm.

The elegance of the definition of Dubinin is the fact that the terms are based on clearly different physical adsorption phenomena of gases occurring in pores with a distinct size. Dubinin's definition was considered to be the most expedient by the IUPAC and has been adopted officially in 1972 [10]. According to these definitions microfiltration membranes are porous media with macropores, whereas mesopores are present in skin layers of anisotropic ultrafiltration membranes. Micropores might exist in RO membranes and are certainly present in zeolites, zeolite filled membranes [11] and certain ceramic membranes [12]. The advantage of coupling the well-established IUPAC nomenclature for the pore types to membrane processes like microfiltration and ultrafiltration is the fact that the strong scientific base which other branches of science (catalysis, material science) have already founded, is joined. Since membrane science is expanding rapidly, more overlap with the other branches will occur (e.g., zeolite filled membranes) and adaptation to the usual terminology is highly desirable.

It is clear that a rough classification of membranes and membrane processes can be made by simply using certain intervals of pore sizes. In some cases, however, a certain overlap exists; e.g., for processes like gas separation, reverse osmosis and pervaporation; so after all the parameter 'pore size' is not a very distinct characteristic. Therefore this classification into pore sizes is often used in combination with other characteristic features (see table 1).

4 Characterization of UF membranes

The major intention of characterization is the prediction of the performance of a membrane from its morphological properties. As mentioned before, this approach requires the use of a model for the pore system and the assumption of a transport mechanism.

There are several reasons for the fact that characterization approaches are not always successful in practice. The problems originate from malfunctions in each of the aspects of characterization:
a). lack of knowledge of the porous membrane structure,
b). disturbing phenomena occurring during filtration, like concentration polarization and fouling,
c). oversimplification of the models used.
Porous media, including UF membranes, usually possess very complicated structures and the models used are gross oversimplifications of the real system. Sometimes it is not even clear

which are the most important characteristics of such a porous structure (see par. 4.2) and, as a consequence, numerical data which should describe the system are not very precise. During filtration difficulties arise as a consequence of the so-called concentration polarization. This phenomenon, which is inherent to all pressure driven membrane processes including pervaporation and gas separation [13], is caused by the accumulation of solute near the membrane surface (figure 3). Only for simple systems concentration polarization can be described exactly as is shown by Van den Berg [14]. The situation will be even more complicated when the solutes involved in the ultrafiltration process have a special interaction with the membrane material (adsorption), or block the pores. Although concentration polarization and fouling is primarily induced by the membrane sieving action, such anomalous behaviour can hardly be predicted by a pore model, simply because the effects are related to the characteristics of the entire system (solution and membrane) rather than to the actual membrane structure only.

Many reseachers [15-17] tried to couple membrane structure and performance. Except for cases where diffusion is the main transport mechanism (dialysis) their efforts had little success. Mason and Wendt [18, 19] suggest a possible reason for these failures: they showed that the commonly used relations between morphology and performance inherently give poor results because the

Table 1. Membrane separation processes and some of their characteristics

membrane process	*pore size*	*other typical characteristics*	*separation mechanism*	*remarks*
microfiltration	5-0.05 μm	isotropic $\varepsilon \sim 10\text{-}50\%$ [1]	size exclusion	
ultrafiltration	50-2 nm	anisotropic $\varepsilon \sim 0.1\text{-}10\%$	size exclusion	for ceramic types $\varepsilon \sim 10\text{-}50\%$
reverse osmosis	1-0.1 nm [2]	anisotropic	solution diffusion	
dialysis	10-0.1 nm	high porosity $\varepsilon \sim 50\%$	effective diffusion	highly swollen networks
electrodialysis	10-0.1 nm	charge density; ζ- potential	difference in charge	
gas separation	< 0.1 nm	anisotropic;	solution diffusion	
pervaporation	< 0.1 nm	anisotropic;	solution diffusion	volatility required

1) porosity ε: for anisotropic membranes the porosity of the top layer and for isotropic membranes the overall porosity is meant.
2) transition between micropores and intermolecular spaces

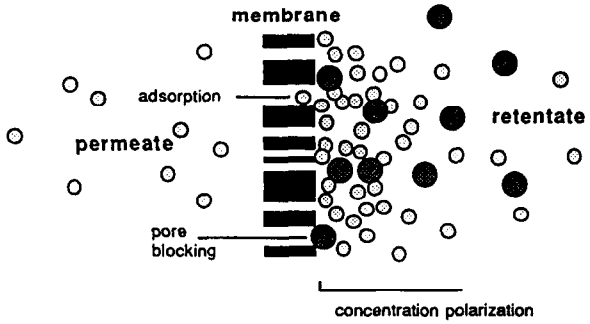

Figure 3. Membrane process (schematic), showing the concentration polarization effect.

mathematical problem is ill-posed. Mason indicated that a performance related parameter cannot predict membrane structure: one specific performance can be reached by more than one membrane structure. Mason's theory is purely based on mathematical modelling and the results are independent of disturbing effects like concentration polarization. So, a performance characteristic can be useful as an indication, but will not give fundamental information of the membrane process or the membrane structure. From this point of view, the determination of, e.g., the membrane cut-off value*) is not a firm basis to predict the performance of real systems but the measurement of structure related parameters should obviously be the first step towards 'total characterization'. The latter can only be reached by using a combination of different morphology and performance related techniques.

4.1 Membrane Characteristics and Characterization Techniques

It is clear that for an appropriate modelling of the performance of a porous structure, starting from the morphology, only the parameters relevant for this specific performance are of interest. For instance, for membrane separation the pore size distribution of the interconnected (or active) pores is the most important feature whereas for catalysis it is crucial to know the overall porosity, the inner and outer surface area, dead-end and interconnected pores.

Whenever morphology related parameters are to be used to calculate experimental properties it is of great importance to characterize the solid in terms which are related to its performance. So, in a model one should take care to use, e.g., a 'pore size' that is relevant for the actual system and the experimental properties that should be described. For this purpose it is convenient to introduce the term 'active parameter' by which the distinct parameter responsible for the experimental properties is meant.

**) the membrane cut-off value is defined in paragraph 4.3.*

Active parameters can only be measured by a limited number of characterization methods. Generally these parameters are highly model dependent and only in an ideal case the characteristic is an 'active parameter' as well as a parameter describing the overall morphology. For instance, from permeability measurements a hydrodynamic (effective) radius can be calculated (par. 5.3), whereas the bubble pressure method of Bechhold (par. 5.3. and [4]) yields the least narrow constriction in the interconnected pore channels of the membrane.

The various methods available to analyse porous structures, measure one or more parameters (related to the method) and all the techniques have their distinct advantages and draw-backs. In paragraph 5 some of the most frequently used characteristics are reviewed, followed by a short discussion on some of the methods that can be used to determine these parameters.

4.2 Morphology Related Parameters

Basic morphology related parameters are summed up in table 2. For an anisotropic membrane, in which the top layer determines the performance, pore size distribution, pore shape (including tortuosity) and top layer thickness are recognized to be complementary parts which should describe all morphological features of the membrane. However, even for simple systems the determination of the parameters mentioned as well as the description of the morphology can turn out to be quite complicated.

Table 2. *Some characteristics of UF membranes*

morphology related parameters	*performance related parameters*
pore size (distribution)	(pure water) flux
pore shape	rejection of solute
tortuosity	specific affinity (for adsorption)
surface porosity	hydrophobicity
top layer thickness	charge density
surface roughness	
surface area	

Pore Size

Despite the superficial simplicity of the term, the concept 'pore size' is not always unequivocal. Proper definition is not only troublesome with respect to pore size and pore shape, but also the 'permeation effectiveness' of a pore is a factor that can cause confusion when different characterization methods are compared. The vague definition of pore size is also due to deviations from the assumed pore shape. Generally pores exhibit quite odd shapes, so not only the cross-sectional 'size' is important (as used in cylindrical models, see fig. 4 A), but also the three

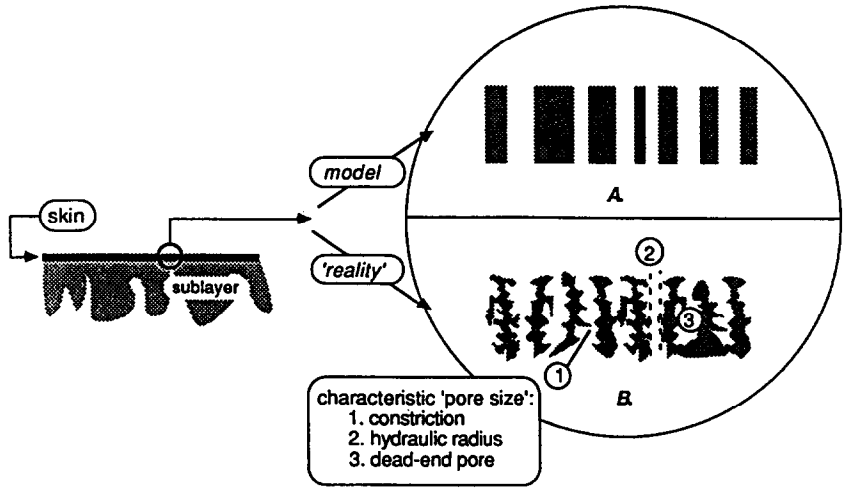

Figure 4. Comparison of ideal model structure (A) and real pore structure (B) in the top layer of an UF membrane.

dimensional pore shape, which influences the resistance of the pore (fig. 4 B). Every model, which couples the membrane structure parameters and the physical phenomena related to that structure, provides a characteristic parameter strictly related to the method and the model (an example has been given in paragraph 4.1).

Surface Porosity

Together with pore size distribution and pore shape, surface porosity is regarded as a very important parameter. With respect to permeability this is only partially true, because the total skin porosity (= surface porosity together with the length of the pore) will determine the membrane resistance. Total skin porosity and surface porosity of a porous medium can deviate to a large extent depending on the structure of the skin, as is illustrated in figure 5.

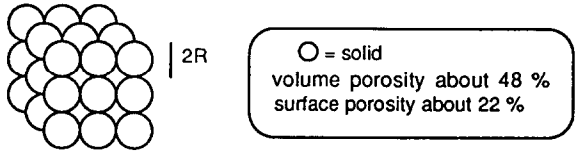

Figure 5. Comparison of surface and volume porosity for a simple model. (simple cubic lattice arrangement of solid spheres).

Surface porosity can have a severe impact on flux decline during the actual filtration process. As Michaels and others pointed out, low surface porosity can aggravate the effect of adsorption and fouling [20, 21]. This is due to a large build-up of solute near the pores. Upon increasing surface porosity, the solute accumulation will be spread more evenly, which also decreases the effect of fouling.

When UF membranes are used as a sublayer for, e.g., composite (bi-layer) pervaporation membranes, surface porosity is considered as a key parameter too. In these applications, it is essential to use a supporting membrane which exhibits small pores, a narrow pore size dsitribution and a high surface porosity.

Surface Roughness

Recently, the importance of surface roughness was shown by Fane et al. [21]. Gekas [22] mentioned the probable significance of surface roughness and hydrophobicity. Scanning electron microscopy revealed that surfaces of UF membranes are microscopically rough ('valley'-'hill' differences between 1 and 20 nm), with the pores usually found in the 'valleys'. Roughness on such a small scale does not only increase the surface area (so there are more possibilities for adsorption), but also deteriorates the hydrodynamics near the surface. The latter promotes the effects of concentration polarization and fouling. The accurate determination of surface roughness is difficult. One of the best methods available today is the correlation of grey levels of electron micrographs to a certain arbitrary degree of roughness. Though the results are very qualitative, the differences found for the limiting cases: rough and smooth surfaces, at least suggest a relation between surface roughness and fouling [21].

Surface Area

Surface area in porous membranes is important for certain membrane applications, such as affinity membrane systems or catalytic membranes. Also in adsorption studies, the surface area is a crucial parameter. In that respect the ratio of pore area and geometric surface area might be important too [20]. A major point is that one should take care to characterize 'the right surface area'. Adsorption is often due to specific affinity of certain species for certain spots on the membrane surface. Generally it is not possible to compare the surface area determined with a reference molecule like nitrogen and that measured with a protein [9]. Since adsorption of nitrogen is of a physical nature, ruled by van der Waals forces, the whole accessible surface area will be measured. Proteins, however, usually are charged (depending on pH) and specific interaction with charges on the membrane surface occurs. Consequently the surface area measured by protein adsorption is related to the number of active sites. On the other hand, measurements with both sorts of molecules can be used to investigate specific adsorption effects.

4.3 Performance Related Parameters

Pure Water Flux

The pure water flux, which is a measure for the hydraulic permeability of the membrane, is undoubtedly the most extensively used parameter in micro- and ultrafiltration. Although the steady state flux during membrane filtration is a main process feature, the pure water flux itself can hardly be seen as an independent membrane characteristic. It is the result of the interplay of pore size (distribution), tortuosity and thickness of the active part of the membrane and will be influenced very much by fouling and concentration polarization of minor components present in 'pure water'.

Rejection and Selective Permeation

Manufacturers tend to characterize membranes by means of rejection measurements with reference molecules like dextrans, proteins or polyglycols. A parameter extensively used is the cut-off value, which is defined as the lower limit of solute molecular weight for which the rejection is at least 90%. It is argued that these rejection measurements have the closest resemblance to operating conditions. Furthermore, the method can be applied simply to actual membrane devices to be used in practical applications. The latter may be true, but the first argument is at least questionable. Rejection measurements, executed with a single solute like a protein or with molecules having a certain weight distribution, always depend on the type of solute, the membrane (system) and the process parameters used. Especially concentration polarization phenomena will effect rejection measurements very much. Consequently, lab experiments and practical situations are not comparable. As a rule, it is not possible to compare rejection measurements done with the same membrane in different types of equipment, and besides that membranes of different manufacturers with the same claimed cut-off value can show a quite different filtration behaviour.

Specific Affinity, Hydrophobicity and Charge Density

Adsorption and fouling are two of the most persistent phenomena causing flux decline. Adsorption phenomena can be understood from interactions between solute and (pore) surface of the membrane These interactions can be of physical nature, e.g, hydrophobic interactions, or originate from specific affinity, e.g., when solute and membrane wall are charged. Arguing that adsorption influences the separation process to a considerable extent, specific affinity might be considered as a performance related parameter. On the other hand, one can regard hydrophobicity and charge density as characteristics of the membrane material, but their ultimate effect depends on the conditions in which the membrane is tested or used.

In affinity membranes [23], a special interaction is necessary for an effective process. The most frequently used (but very empirical) way to investigate specific affinity, is by measuring the adsorption of relevant adsorbate-adsorbent pairs. A more fundamental approach concerns the

analysis of the molecular groups at the surface of the membranes by, e.g., ESCA, SIMS, NMR or IR-spectroscopy. Such approaches are very time consuming and results mostly are difficult to interpret [24].

Hydrophobicity is suggested to be a very important parameter in membrane fouling and it is expected that a more hydrophobic surface will exhibit a higher degree of fouling. A number of researchers have tried to find a way to express hydrophobicity in a quantitative way. Contact angle measurements are routinely used for dense, flat surfaces but these values cannot be extended to membranes which have a rough surface and contain pores [25, 26]. Recently two methods for the measurement of the 'critical surface tension'*) have been published [27, 28]. Although the physical background of these methods is not very clear yet, results do correlate relatively well with expectations concerning grades in degree of hydrophobicity. Despite the extensive research on the subject, the direct relation between hydrophobicity and membrane fouling has not been proven yet. Presumably not only hydrophobicity, but also the interaction between charges present on the membrane surface and the charged species in solution is of great practical importance.

Depending on their molecular structure, membrane surfaces can contain different types of charged spots. But even without such special entities, membrane pore surfaces carry a definite charge [30]. Several species that have to be separated by UF, like proteins, are charged too. In such a case the performance of the membrane will be strongly influenced by the interaction between membrane and solute. The ζ-potential of the membrane, which is correlated with the surface charge of the pores in the membrane, can be measured fairly simply by streaming potential or electro-osmosis measurements [31, 32]. The influence of the interaction between the membrane and the charged solute particles as well as that between particles during filtration can only be described in a semi-quantitative way [14, 33].

5 Characterization Techniques

Table 3 shows a number of characterization methods which are presently available. Some of these are still under development, and therefore not (yet) suitable for routine characterization. The majority of these techniques have not been developed specifically for membrane characterization and the interpretation of the results found by these methods needs special care.

**)The term 'critical surface tension' is strictly related to the surface tension found using the concept of Zisman [29]. In the case of the 'sticking bubble method' [27] the term 'critical bubble adhesion tension' would be more appropriate.*

Table 3. Characterization methods and characteristic parameters

method	*characteristic*	*remarks*	*M / P*
gas adsorption-desorption	pore size distribution BET area	dry samples	M
electron microscopy	top layer thickness surface porosity pore size distribution qualitative structure analysis	surface (pore) analysis	M
flux measurements	hydraulic pore radius 'pure water flux'		P
rejection rejection selective permeation	cut-off value		P
bubble pressure method liquid displacement method	pore size distribution	active pores	P/M
mercury porosimetry	pore size distribution	dry samples, measurement of the pore entrance	M
thermoporometry	pore size distribution pore shape	wetted samples	M
permporometry	pore size distribution	active pores	P/M

P: permeation related parameter
M: morphology related parameter

5.1 Gas Adsorption-Desorption

This technique can be considered as a standard method in the material science of porous ceramics and catalysts. It is based on the analysis of Thompson (Lord Kelvin) who described the thermodynamics of curved surfaces already in 1855. The theory implies the lowering of the saturated vapour pressure of concave liquid interfaces in comparison with that of a flat surface of the same liquid. This means that inside small pores a gas can condense to a liquid at relative pressures lower than unity. Zsigmondi was the first who used this effect to measure pore sizes and introduced the 'capillary condensation theory' [9].

Gas adsorption isotherms express the relationship between the amount of gas adsorbed, at constant temperature, and the relative pressure. Many (meso)porous systems exhibit a distinct adsorption-desorption behaviour which leads to a characteristic so-called 'type IV-isotherm'. Such isotherms possess a hysteresis loop (fig. 6).The origin for the hysteresis effect lies in the different geometrical factors which rule the adsorption and desorption process in a mesoporous substrate.

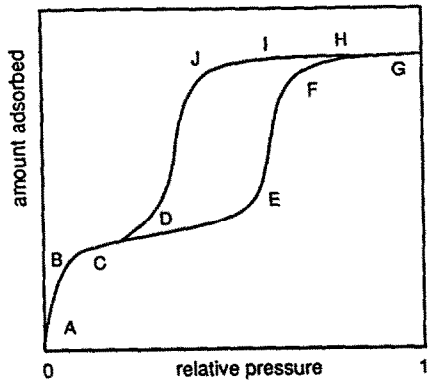

Figure 6. Type IV-isotherm; adsorption branch ACDEFG, desorption branch GHIJDB.

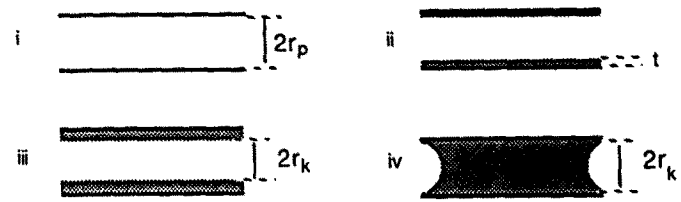

Figure 7. Several steps in the adsorption analysis: i to iv for increasing relative vapour pressure, iv: capillary condensation has occurred r_p: pore radius, r_k: Kelvin radius, t: t-layer thickness. Steps are in connection with figure 6: i <--> A, i and ii <--> BCDE and iv <--> EFG; GHI.

The adsorption-desorption process can be imaged as follows. Due to dispersion forces gas molecules adsorb on the surface of a porous material but this adsorption is restricted to a thin layer on the wall (fig. 6: route ABC). The adsorbed molecules are in thermodynamic equilibrium

with the gas phase above the surface and the amount adsorbed is determined by the relative pressure of the gas and the curvature of the interface. At increasing pressure more molecules are adsorbed and layers of adsorbed molecules on the wall form a new liquid-gas interface (fig. 6: point D; fig.7, iii). Because of the curved interface, the vapour pressure of the liquid is lowered. As the curvature of the meniscus passes a certain critical point, pores with a size strictly related to the curvature of the liquid, are filled very quickly: capillary condensation occurs (fig.6, point E). As the pressure is progressively increased the larger pores are filled too (fig.6, EFG).

During desorption the reverse process occurs. At a high relative pressure all pores are filled (fig. 6: GHI) and the equilibrium is governed by the curvature of the meniscus of the liquid at the pore

entrance. When the relative pressure is lowered, nothing will happen until the pressure comes below the equilibrium value (given by eq. 1) and the liquid evaporates emptying the entire pore (fig.6, region JD).

When the adsorbed molecules are regarded as a 'normal' fluid with a liquid-gas (l-g) interface, the equilibrium vapour pressure will be determined by the curvature of the (l-g) interface. The most elementary relation in this analysis is the Kelvin equation (1).This relation is applicable for pore sizes between about 1 nm and 50 nm, although there is some discussion about the lower limit [7, 9]. The upper limit is set by the experimental difficulty to measure at relative pressures close to unity, e.g., when nitrogen is used as condesable gas, a pore size of 50 nm corresponds with a relative pressure of 0.98.

$$\ln p_r = (-\gamma v / RT) \cos\Theta * (1/r_{k1} + 1/r_{k2}) \qquad (1)$$

p_r : relative pressure (-)
γ : interfacial tension (N/m)
v : molar volume liquid (m^3/mol)
Θ : contact angle (°)
r_{ki}: Kelvin radii describing the curvature of the interface (m)

For capillary pores, with radius r, this equation reads:

$$\ln p_r = (-\gamma v / RT) \cos\Theta * (a/r_k) \qquad (1')$$

with: a = 1 during the adsorption and a = 2 for the desorption process

One has to realize that the radius (r_k) given by the Kelvin equation (1') is the radius of the pore (r_p) minus the thickness (t) of the adsorbed layer (fig. 7), hence:

$$r_p = r_k + t \qquad (2)$$

with: r_p = pore radius (m)
t = thickness of the adsorbed layer (m).

This t-layer thickness has to be determined from adsorption measurements on a flat reference surface. Although in principle incorrect, it is generally accepted to use the t-layer thickness found for silica or to interpolate the t-layer thickness from the experimental data found on the porous sample itself [9].

During adsorption and desorption the curvatures of the gas-liquid interface are usually different (which in equation (1') gives rise to the different values for a). Consequently, the condensation and evaporation processes are not the exact reverse of each other and hysteresis arises. The path of this hysteresis curve permits one to work out models about pore structure and shape. Several examples are represented in table 4 and figure 8 [9].

In the gas adsorption-desorption theory the interaction between the solid and the gas is assumed to be very low. But in practice the quantitative description of the adsorption process appears to be

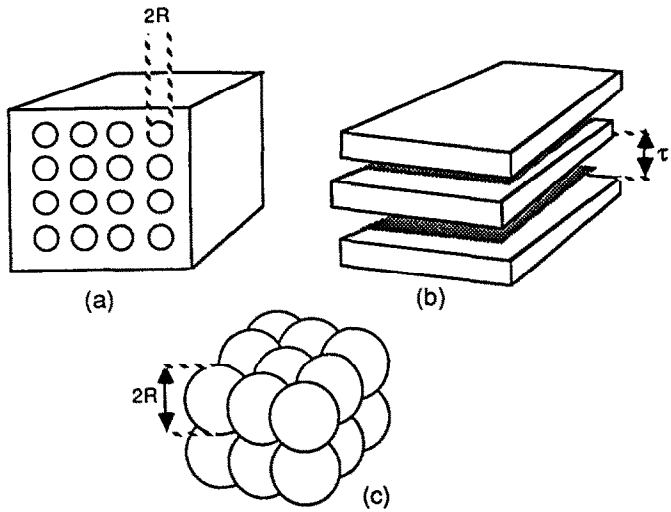

Figure 8. Some idealized pore structures showing different adsorption-desorption hysteresis, (a) non-intersecting capillaries, (b) parallel plates and (c) packed spheres; see also table 4.

Table 4. *Kelvin radius r_k (in eq. 1'), during the desorption process, compared to pore size characteristics of ideal pore systems (see also figure 8)*

system	*size parameters*	*relationship with r_k and a (eq.1)*	
non-intersecting cylindrical capillaries	radius of cylinder = R	a = 2	$r_k + t = R$
parallel plates	slit width = τ	a = 1	$r_k + t = 0.5\,\tau$
packed spheres	sphere radius = R	a = 2	
cubic packing			$r_k + t = 0.414\,R$
rhombohedral packing			$r_k + t = 0.229\,R$

influenced by very small differences in interaction energy. Therefore the use of standard adsorption plots determined for a number of classified adsorbent-adsorbate systems, showing different interaction energies, was proposed by Lecloux [34]. However, fundamental aspects in a theoretical as well as in a practical sense are still under development [34].

Ceramic membranes can be characterized relatively simply by adsorption-desorption techniques, as shown by several researchers [34, 35]. These membrane systems are quite comparable to the standards used in catalysis (alumina and silica) and the porosity is high enough to cause a measurable effect. In figure 9 the pore size distribution of a ceramic γ-alumina membrane is

shown. Figure 10 gives an example of the very distinct pore size distribution found for polymeric poly(2, 6 dimethyl-1,4 phenylene) oxide membranes. The latter is one of the few illustrations of pore size measurements of polymeric membranes by the gas adsorption-desorption method published [36-38]. This is probably caused by the low surface porosity which is usually observed for anisotropic polymeric UF membranes (see table 5). It is also possible that the pore shape is such that capillary condensation is not found or not recognized [9]. Furthermore, the adsorption-desorption analysis of polymers is relatively unknown and phenomena like swelling, caused by the vapour used, sometimes do occur. [9, 34].

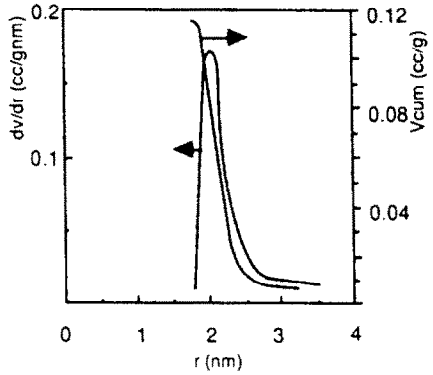

Figure 9. Pore size distribution found for γ-alumina membranes using gas adsorption-desorption [3].

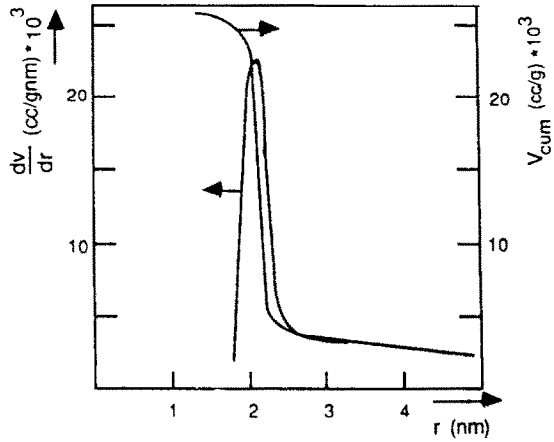

Figure 10. Results of adsorption-desorption measurements applied to PPO membranes [36].

A general draw-back of the adsorption-desorption method is that the samples have to be dried before the analysis. Therefore the membrane is in a different situation compared to that in the filtration process. Due to capillary forces occurring during the drying process, the porous

structure may be damaged. Alterations of the structure can also be caused by the de-swelling of the membrane matrix. As a rule, polymeric membranes will be more susceptible to these effects than ceramic membranes.

5.2 *Electron Microscopy: Qualitative Overall Structure Analysis, Surface Porosity and Top Layer Thickness*

Electron microscopy is often used for the observation of membrane structures. Morphological features of microfiltration membranes and, to a lesser extent, of UF membranes can be inspected relatively easily. Especially the Scanning Electron Microscope (SEM) is very suitable for this kind of systems. The ultimate resolution of SEM is about 5 nm which is sufficient for qualitative structure analysis and since the depth of field is high ($\approx$ 150 μm), sharp images of relatively rough surfaces can be obtained. A Transmission Electron Microscope (TEM) in principle has a higher resolving power ($\approx$ 0.3 nm) than SEM has, but the depth of field is only 2 μm (at higher magnifications even smaller). Besides that, very special preparation methods have to be used to make a sample suitable for TEM [39, 40].

In general, the investigation of UF membrane structures by electron microscopy is a delicate and difficult work. This is caused by a number of problems, which in fact, together with the resolution, depth of field and the structure of the sample itself, set the limits of the electron microscopic techniques and determine the suitability of the methods. Furthermore, the interpretation of micrographs may be difficult, analysis is only local and processing of the data may be very time consuming. Some explicit problems are:

1. pores at the surface can be isolated ('blind') and not connected to the porous network.
2. the resolution of the method is too low to detect very small pores.
3. preparation techniques can create artefacts which have a large impact on the final result.

Porous materials are known to be very sensitive to preparation steps such as drying and de-swelling which both can introduce defects in the native membrane structure. These problems are very well known in the biological and medical field and a large number of preparation techniques have been developed to preserve the sample in a state that resembles its native state as closely as possible. One of the newest techniques in this field is cryo-preparation which allows the examination of the membrane structures in the (water-) swollen state. In a microscope (SEM or TEM) equipped with a cryo-unit, preparation as well as examination of the sample at low tempertures is possible (typically -130 °C) [39-41]. The critical step in this preparation method is the freezing of the sample. The cooling rate should be so high that the water is fixed in a glassy state, crystallization should be avoided because this can alter or destroy the structure.

Surface Porosity

The only method which is suitable for the direct estimation of surface porosity is electron

microscopy. A major draw-back is that microscopic analysis is very local and that the resolution is insufficient to study finely porous structures. Also, the method becomes very laborious when a reasonable level of precision has to be reached because it is necessary to count and measure a large number of pores. The processing of the data is time consuming, although computer aided image analysis can be used [42]. Consequently, quantitative values of the surface porosity are not much used in practice. The data that are available indicate a very low porosity (0.05-1 %) for the majority of UF membranes, see table 5 [42-49].

Table 5. Surface porosity values from literature

membrane type and cut-off value (D)	r_p *(nm)*	*r(min-max) (nm)*	*n* $(1/m^2)$	ε_{surf} *(%)*	*method*	*ref.*
XM 100A / 10^5	9	5-12	$30*10^{12}$	0.75	TEM (a)	42
XM 300 / $3*10^5$	12	6-19	$6.7*10^{12}$	0.3	TEM (a)	42
XM 300 / $3*10^5$	12		10^{14}	4.7	TEM (b)	42
Millipore PTSG PSf / 10^4	3	1-15	$4*10^{15}$	7-12	TEM	43
Millipore PSED / $25*10^3$	15	4-75	$2.2*10^{12}$	0.3	TEM	44
XM 50 / $5*10^4$	4	1-12	$5*10^{12}$	0.04	TEM	44
XM 100 / 10^5	7	2-30	$3*10^{12}$	0.54	TEM	44
Millipore VF (10nm)	19	9-70	$2*10^{12}$	0.25	TEM	44
PM 30 / $3*10^4$	6		$2*10^{12}$	2	TEM	45
YM 30 / $3*10^4$				50	TEM	45
UM 10 / 10^4	0.5	0.3-0.8	10^{16}	2.5-4	rejection/flux	46
PM 10 / 10^4	0.8	0.5-1	10^{16}	20	rejection/flux	46
PVDF		3-4	$2*10^{15}$	10	liq. porometry	47
PSf, DDS GR61PP		15-19	10^{14}	1	SEM	48
polyimide UF membranes		1.5-6	$(1\text{-}0.1)*10^{15}$	0.7-0.9	TEM	49

r_p: average pore radius (a): angle sputtered ε_{surf}: surface porosity

n : number of pores (b): rotary sputtered

It has also been tried to calculate the surface porosity from data found with other characterization techniques. Examples of this approach are the combination of rejection and flux measurements [46] or the liquid-liquid displacement technique and SEM [47]. Starting from the pore size, combined with permeability measurements and assuming a certain skin thickness, tortuosity and pore shape, the number of pores and the surface porosity is calculated. Again the final result will depend strongly on the parameters assumed (and determined) and the model used.

Top Layer Thickness

Top layer thickness is one of the parameters frequently estimated from electron microscopic pictures. This can give only a rough estimate because the sizes of the pores, present in the top layer, are below the detection level of the EM technique. Also the fact that a distinct transition from top layer to support often does not exist, makes a straightforward analysis impossible.

A new approach to determine the skin thickness of anisotropic UF membranes is based on the penetration of colloidal particles of a well-known size and a very narrow size distribution into the macroporous sublayer of an anisotropic UF-membrane [50]. The particles entering from the macroporous sublayer side, penetrate into the porous support until small pores near or in the skin are reached. When the pore size is smaller than the particle size the particles will get stuck. When the particles used are only slightly larger than the pores in the skin, a thin layer not permeated by colloids is formed. The thickness of this layer can be measured by applying scanning electron microscopy (SEM) in two different modes: the secondary electron image (SEI) and the backscattered electron image (BEI) mode. Micrographs made in the SEI mode are essentially topographical, the rough morphological structure can be examined. The backscattered mode yields not only topographical but also analytical information about the specimen. In the BEI mode the contrast depends on the atomic number of the materials present in the membrane: the gold particles are detected as light areas in the dark polymer matrix. The skin thickness appears as a dark area between trapped gold particles and a sputtered gold layer on top.

Figure 11 a and b show cross-sections of PPO membranes treated with colloidal gold solutions containing particles with a mean diameter of 6 nm and 50 nm respectively. The right hand side of the picture shows the membrane in the SEI mode. It can be seen that the sample is fractured very sharply, as is essential for a correct interpretation of the picture. The presence of gold can be detected very well in the backscattered mode (BEI, left hand side of figures 11 A and B). Although the individual particles cannot be detected, the edge formed by these permeated particles can be seen clearly. In the BEI mode, three layers can be recognized: a thin light line resulting from sputtered gold on top of the membrane, a more diffuse layer caused by the penetrated particles and in between the (dark) skin layer in which the pores are smaller than the sol particles. When a PPO membrane is treated with a sol, containing particles of 6 nm, an impenetrable layer with a thickness of about 0.2 μm is detected. Using a sol with particle size 50 nm the thickness of the toplayer is varying between 0.2 and 0.3 μm, a very small increase compared to the

experiments where 6 nm particles were used. This indicates that PPO membranes have a very well-defined skinlayer thickness, with a pore size very much different from the pores in the macroporous layer underneath.

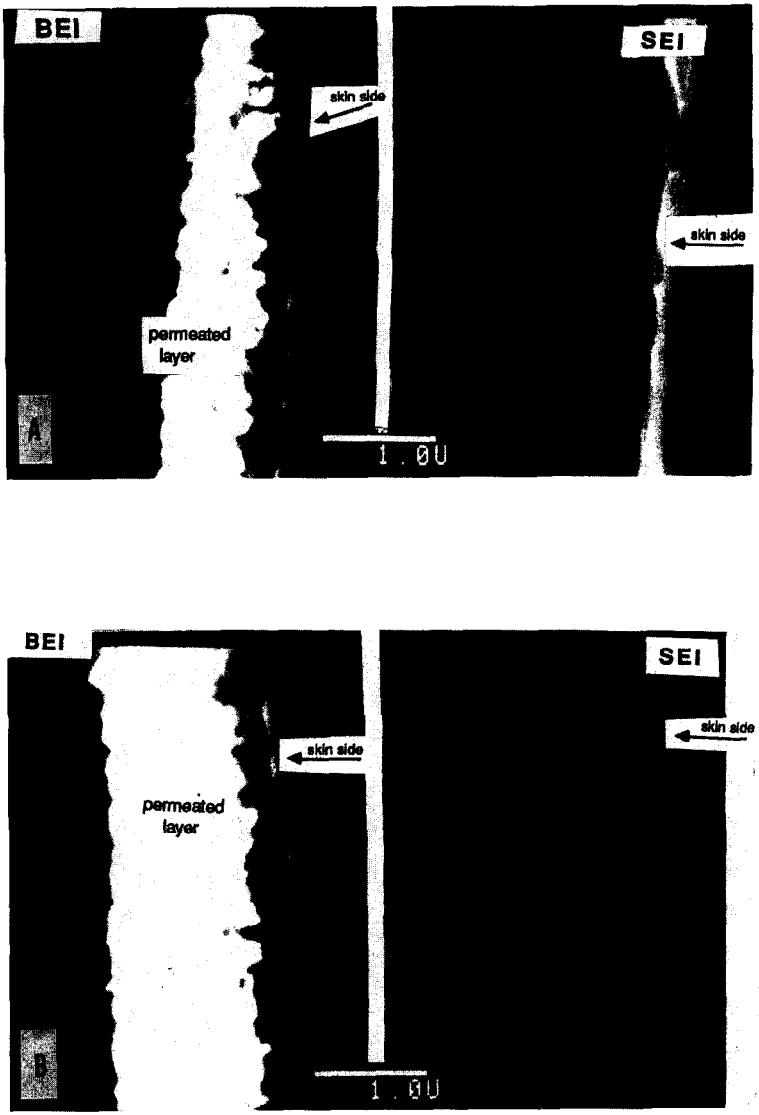

Figure 11 A Cross section of a PPO membrane, using BEI (left-hand side) and SEI (right-hand side) modes, permeated with gold sol solution; average colloid particles diameter 6 nm.
Figure 11 B. ibid, average colloid particle size 50nm. In both figures the cross sections have been tilted slightly to make the sputtered layer more visible [50].

5.3 *Permeability Measurements, Bubble Pressure Method and Liquid Displacement Technique*

Permeability

Permeability of a membrane for a certain liquid as such can be considered as a characteristic parameter; often a so-called hydraulic radius is calculated from the measured fluxes. In such an analysis, the permeability is determined, the porosity ε, the tortuosity τ and the membrane thickness l are estimated (or preferably determined) and subsequently the pore size can be calculated from the Hagen-Poiseuille equation (3).

$$J = P * (\Delta p / l) \qquad (3)$$

with: $$P = n \pi r^4 / 8 \eta\tau \qquad (3')$$

J = flux (m/s)
P = permeability (m^3s/kg)
n = number of pores ($1/m^2$)
η = viscosity (kg/ms)
l = membrane thickness (m)
Δp = pressure difference across the membrane (N/m^2)
τ = tortuosity (-)

It is obvious that such an approach depends largely on the model as well as on the estimated values used. Also, the model cannot discriminate between a system with few large pores and one with a large number of small pores (when, of course $n r^4$= constant).

The method can be improved by using a gas as the permeating medium instead of a liquid. As the transport mechanism for gases is dependent on the overall pressure in the system and the pore size, discrimination between fine and coarse porous media is possible when the permeability at different pressures is measured. An accurate quantitative description of such systems and therefore the calculation of the hydraulic radius is still ambiguous [51].

Bubble Pressure Method and Liquid Displacement Technique

The bubble pressure method, introduced by Bechhold in 1908, is based on the measurement of the pressure necessary to blow air through a water-filled porous membrane (figure 12). Using Cantor's equation (4) a pore size can be calculated.

$$r = 2 \gamma \cos \Theta / \Delta p \qquad (4)$$

where: r = radius of the capillary (m)
γ = surface tension (water/air) (N/m)
Θ = contact angle (°)
Δp = pressure difference across the membrane (N/m^2)

Usually complete wetting is assumed, i.e., $\cos \Theta = 1$.

In its most simple form, the moment at which the first bubbles appear, 'the bubble point', is determined visually. The pore size that is related to this 'bubble pressure' represents the largest pore present in the membrane.

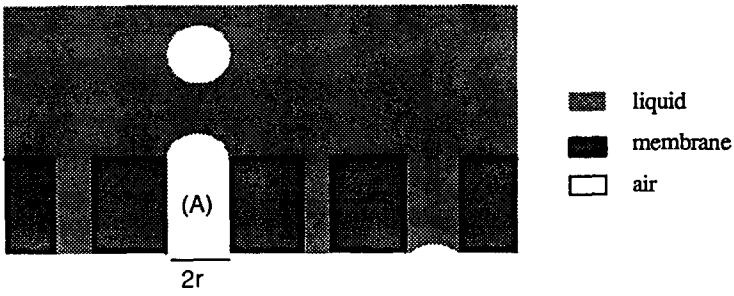

Figure 12. Principle of the 'bubble pressure technique'. In pore (A) the bubble point has just been reached, eq. (4) holds.

When the method is applied to MF membranes with pore sizes between 1.5 and 0.15 μm, typical bubble pressures are between 0.1 and 1 MPa. For UF membranes with pores that are much smaller, higher pressures (about 10MPa) are necessary. At these pressures the membrane matrix will deform and the structure will be altered, which will consequently lead to erroneous results. To avoid this, Bechhold and Erbe [52] used penetrating systems consisting of two immiscible liquids, which exhibit a low interfacial tension. For the immiscible pair isobutanol/water an interfacial tension of 1.85 mN/m at 20 °C is found and the system water/isobutanol/methanol(25/15/7 v/v) exhibits an interfacial tension of 0.35 mN/m [52]. With the latter system pores of about 1.5 nm are already 'opened up' at pressure differences of 0.5 MPa.

When this so-called 'liquid-liquid displacement technique' is combined with the permeability method, a pore size distribution rather than the largest pore of the medium is found. For such permeability measurements a set-up similar to the one used for bubble point measurements is used, but now the applied pressure and the flux through the membrane are measured simultaneously. Transport through a pore will start at the moment that the first liquid is displaced by the second one, i.e., at a pressure difference given by equation (4). Once the pore is open, transport will increase upon increasing the pressure difference as described by equation (3). Using a capillary model together with a proper estimation of tortuosity and the thickness of the membrane (or the skin layer thickness), the number of pores can be calculated.

Co-workers of Bechhold found that the observed pore sizes depend on the rate of pressure increase. The faster the pressure was raised, the smaller the measured 'pore size' values appear to be. Schlesinger attributed this effect to the viscosity of the two phases [52], but although he corrected equation (3) for this effect, the resultant relation did not completely account for all the deviations from the ideal case. It might be that a wetting phenomenon effect disturbs the measurement [53, 54]. This means that it is not sufficient to determine the 'bubble-pressure

curve' of the membrane, but one should also correct for incomplete wetting.

Another disadvantage of the liquid displacement technique is that polymeric membranes may swell or shrink in the alcohol-water system (compared to pure water). As Nikitine pointed out [55], this influences the measured pore sizes. To get an impression of the effect, several permeating media causing a different degree of swelling, should be used. Anyway, the often used argument that during these measurements, the membrane should be in an environment close to 'real' filtration condition does not hold.

To increase reproducibility and accuracy of liquid displacement measurements, researchers nowadays use high precision devices and computerized set-ups [56, 57]. Especially for the UF membranes these are substantial improvements, which permit measuring conditions close to equilibrium so corrections in the sense of Schlesinger [52] are not necessary anymore. Also the technique becomes more suitable for standard measurements.

5.4 Mercury Porosimetry

This technique has the same basis as the bubble pressure method: the Cantor equation (eq. 4). But as mercury is a non-wetting liquid, Θ will be higher than 90°. A widely accepted value for Θ is 140°. Originally, mercury porosimetry was mainly used for the characterization of macroporous structures. The technique itself consists in the measurement of the volume of mercury which is forced into the pores of an evacuated porous sample. As the method is simple, it enjoys great popularity among ceramic material scientists. Unfortunately, the method is hardly applicable for UF membranes, since pressures are very high for pores in the nanometer range. A pore of 4 nm corresponds to a pressure of ≈200 MPa, a pressure which may damage ceramic UF membranes and surely will densify the structure of polymeric membranes [58, 59].

5.5 Thermoporometry

Thermoporometry, introduced by Brun and Eyraud [35, 60, 61], is based on the microcalorimetric analysis of solid-liquid transformations in porous materials. Since the system of water-filled pores has the closest resemblance with the practical situation of membrane filtration, the solid-liquid transition of water is used for the pore size analysis. Due to the strong curvature of the solid-liquid interface present within small pores, a freezing (or melting) point depression of the water (or ice) occurs. According to this concept, the size of a confined ice crystal (which is set by the size of the pore), is inversely proportional to the degree of undercooling, whereas the pore volume is directly related to the apparent transition energy. With a differential scanning calorimeter (DSC) the transition can be monitored easily.

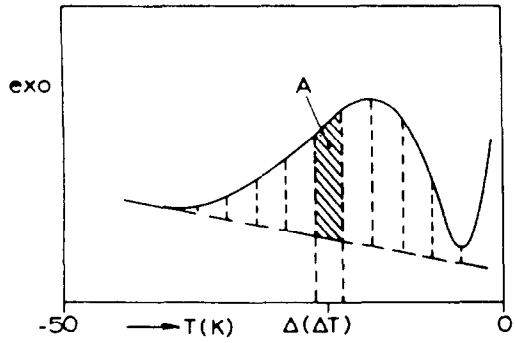

Figure 13. Schematic representation of the heat effect measured from the melting of a liquid in a porous medium as a function of temperature.

The melting diagram (fig. 13) can be monitored in a differential scanning calorimeter (DSC) and the relation between the pore size r (nm) and the extent of undercooling $\Delta T = T - T_0$ is obtained with the help of the equations derived by Brun [60, 61]. For cylindrical capillary pores, with water inside, it leads to:

during solidification: $r = (-64.67/\Delta T) + 0.57$ (5a)

and during melting: $r = (-32.33/\Delta T) + 0.68$ (5b)

The area between T and T+dT (figure 13) represents the heat effect of the melting of the ice crystals in the pore size between r and r+dr. From this heat effect (in Joules) the pore volume of the pores with sizes between r and r+dr is calculated with the help of equation (6a) which gives the heat of melting W_a (in joules per gram) as a function of the undercooling (ΔT) for pure water [60].

solidification: $W_a = -5.56.10^{-2}\,\Delta T^2 - 7.43\,\Delta T - 332$ (6a)

melting: $W_a = -0.155\,\Delta T^2 - 11.39\,\Delta T - 332$ (6b)

The differences between the solidification and the melting process in *cylindrical* pores, expressed in the two sets of equations, are due to the fact that the phase transitions are not ruled by the temperature only, but also by the shape of the interfaces present during the transition. In shere shaped pores this difference does not exist, and consequently both transitions (s-->l and l-->s) are described by equation 5a and 6a. In fact, thermoporometry can actually be used to decide whether a structure contains spherical or cylindrical pores.

The results found for the two systems alumina and PPO, shown in figure 14 and 15, suggest that thermoporometry and gas adsorption-desorption are compatible techniques. Brun [60], however, pointed out that this is only true for non-swelling systems.

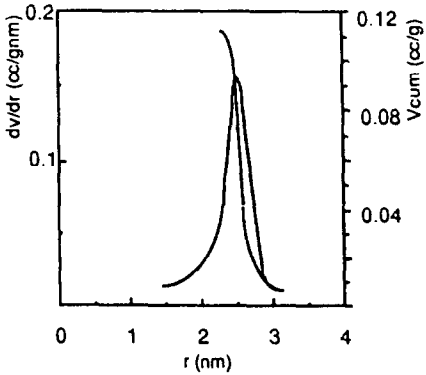

Figure 14. Pore size distribution of an alumina membrane found with thermoporometry.

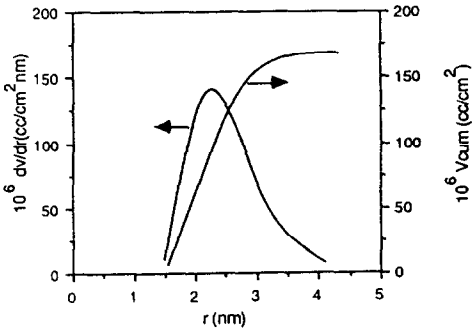

Figure 15. Pore size distribution of a PPO membrane found with thermoporometry.

5.6 Permporometry

Permporometry is a relatively new technique by which the size distribution of the active pores of an UF membrane can be measured [61-65]. The technique is based on the controlled blocking of pores by condensation of a vapour, present as a component of a gas mixture, and the simultaneous measurement of the gas flux through the membrane. The capillary condensation process is related to the relative vapour pressure (see: Kelvin relation (eq. 1)), so exact control of the relative vapour pressure permits stepwise blocking of pores. Starting from a relative pressure equal to 1, all the pores of the membrane are filled, hence unhindered gas transport through the membrane is not possible. When the vapour pressure is reduced, pores with a size corresponding to the vapour pressure set, are emptied and become available for gas transport. By measuring the gas transport through the membrane upon decreasing relative vapour pressure, the size distribution of the active pores can be found.

The calculation of the number of pores in the membrane requires a well-defined transport regime. It is known that transport phenomena of gases through systems containing nanometer-sized pores sometimes are extremely diffucult to describe [51, 68]. Especially when a mechanical pressure gradient is present, the diffusional and convective mechanisms interfere in a very complex way [68]. These difficulties make the use of the set-ups as described by Eyraud [61] and Katz [62] less suitable for pore structure modelling. The relation between pore structure and transport properties is more easy to model when a so-called counterdiffusion approach (i.e., Knudsen diffusion [3]) is used. In such a set-up the driving force for transport is a concentration gradient of the inert gases, so that only gas diffusion accounts for the transport through the membrane. The principle of this method is given in figure 16. In this set-up the driving force for transport is

a concentration gradient of oxygen and the diffusive transport is measured as an increased oxygen concentration in stream 1. The condensable gas, methanol, is used at a uniform relative vapour pressure all over the system. The relative vapour pressure of methanol determines the number of open pores available for oxygen diffusion. Since the gas transport is related directly to the open, active pores with radii (for UF membranes), generally in the order of nanometers, it can be assumed that the diffusion is of the Knudsen type. In case of a capillary model this can be described by equation (7).

$$J_k = \{ \pi n r_k^2 D_k \Delta p_{gas} \} / \{ R T \tau l \} \qquad (7)$$

$$D_k = \{0.66\, r_k\, (8RT / \pi M)^{0.5}\} \qquad (7a)$$

J_k : diffusive flux (mol/m^2)
n : number of pores (/m^2)
r_k : Kelvin radius (m)
D_k: Knudsen diffusion coefficient (m^2/s)
Δp_{gas} : partial pressuregradient of oxygen (N/m^2)
τ : tortuosity (-)
l : skin thickness (m)
M : molar mass permeating gas (g/mol)

For the principle of capillary condensation used here all the features mentioned before (in par. 4.1) are valid. So, in principle, all the adsorption and desorption processes are not occurring in the pore itself, but in a pore with an adsorbed t-layer, i.e., in the 'core'. For the calculation of the real pore size, the thickness of the t-layer should be known (equation 2).

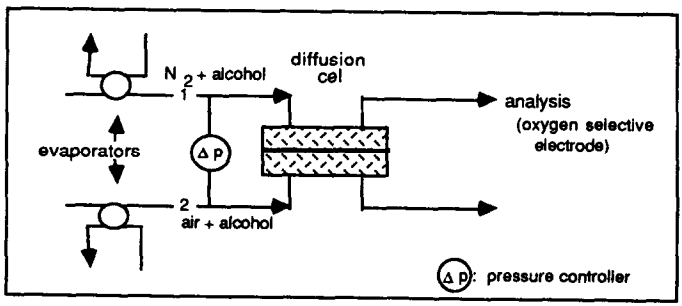

Figure 16. Permporometry: experimental set-up; explanation see text.

A typical example concerns the calculation of a pore size distribution of a PPO membrane. From the plot of the diffusive flux vs the relative vapour pressure, given in figure 17, and using relation (1) the Kelvin radius (r_k) is found from the relative vapour pressure value whereas the number of pores is calculated from the experimental flux (using equation 7). To calculate the real pore radius (r_p), the Kelvin radius has to be corrected for the adsorbed t-layer (equation 2). In classical adsorption studies this thickness is calculated from separate adsorption experiments which are performed using homogeneous non-porous surfaces [7]. This approach is very laborious and therefore an approximation is used to calculate the t-layer directly from the permporometry data, as follows.

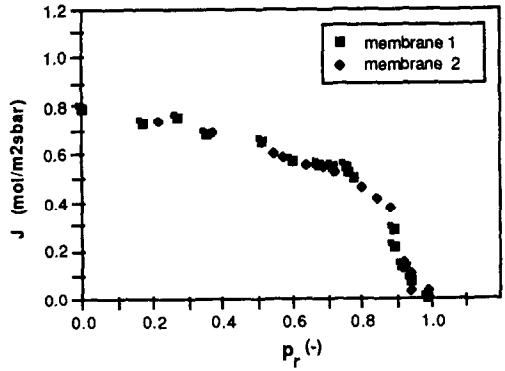

Figure 17. Diffusional oxygen flux as a function of relative vapour prerssure during adsorption, for two different membrane samples. The samples were both made from the same polymer solution and in the permporometry experiments, methanol was used as the condensable gas.

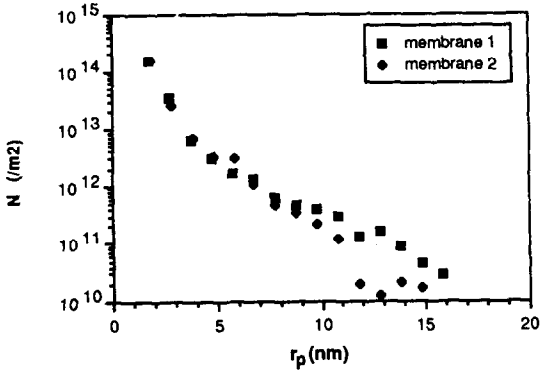

Figure 18. Size distribution of interconnected pores in two samples of PPO membranes (same samples as in figure 17).

The validity range of the Kelvin equation, 1.3 nm < r_k < 50 nm, corresponds with relative vapour pressures of 0.60 < p_r < 0.99. From figure 17 it can be seen that the flux is increasing rapidly upon lowering p_r (below $p_r \sim 0.9$) and up to $p_r = 0.6$ the flux is growing relatively fast. At lower relative pressures the flux does increase, but not very much. It can be argued that in the range of relative pressures between 0.99 and 0.6 capillary desorption takes place: the flux increases because of an increasing number of open pores. At lower relative pressures only the t-layer in the open pores desorbs, so the pore size available for transport becomes somewhat larger and again the flux increases. When it is assumed that the flux increase at lower relative pressures ($p_r \leq 0.6$) is only due to the desorption of the t-layer and that in all the pores present the t-layer thickness is equal we can calculate this thickness (t) using equations (2) and (7). At the relative pressure of 0.6 the pore size available for transport is r_k and when the t-layer has been totally desorbed (at $p_r = 0$) the

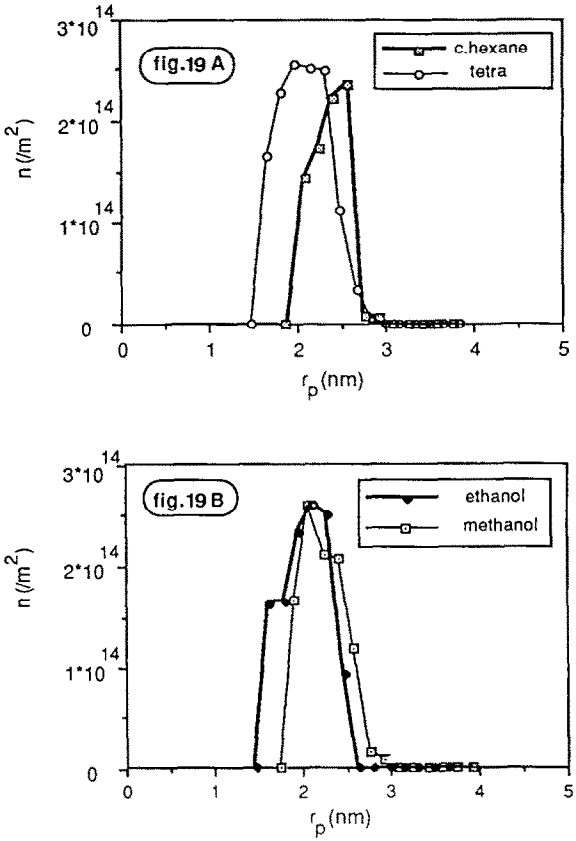

Figure 19 A and B. Pore size distributions of active pores of γ-alumina membranes measured with different adsorbents in permporometry.

effective pore size is $r_p = r_k + t$. So starting from the experimental flux values found in figure 17 at $p_r = 0.6$ and $p_r = 0$ respectively, and using equation (2) and (7), the value r_p ($= r_k + t$) for each pore can be calculated and hence t is obtained. Of course this method yields only a quite rough estimation of the t-layer thickness, but since in the case of PPO membranes larger pores are determining the performance of the membrane, it is sufficient to know that this thickness t is very small. For methanol, the condensable gas used here, in this way a t-layer thickness of 0.25 nm was found, a value that agrees fairly well with data in literature [3, 7, 65]. The resulting pore size distribution is given in figure 18. The fore-going approach can be applied to different membrane-adsorbate systems, and different thicknesses are found (table 6; [3]), the resulting pore size distributions, however, are not changed, as is shown in figure 19.

Table 6.Thicknesses of the t-layer found for different membrane-adsorbate couples [3]

membrane	*adsorbate*	*t-layer thickness (nm)*
γ-alumina	methanol	0.7
	ethanol	0.4
	cyclohexane	0.5
	carbon tetrachloride	0.4
PPO	methanol	0.25
	ethanol	0.5

5.7 Rejection, Selective Permeation and Fouling

As already mentioned before, rejection measurements are often seen as the 'standard' characterization method. Since phenomena like concentration polarization, pore blocking and fouling will interfere severely with selective permeation measurements, the analysis is less suitable for fundamental characterization purposes. Only by choosing special circumstances, a better defined process may be established and conclusions in relation to the pore structure are possible.

Diffusion processes, the main transport mechanism in, e.g., dialysis, are well-defined and concentration polarization will only have a minor effect on membrane performance (because diffusion through the membrane is a relatively slow process). Klein [15] has shown that hemodialysis membranes can be characterized by simple diffusion models. Bohrer [65], on the other hand, tried to use diffusion measurements to characterize Nuclepore membranes, but still had to account for boundary layer effects.

Recently, Hanemaaijer [48] introduced a method for estimating an effective pore size from rejection measurements of low molecular weight saccharides. Because the rejection of such species is low, concentration polarization is supposed to be negligible. The elegance of the method is that it is reasonably simple to use and that it is possible to measure clean, fresh membranes as well as fouled membranes. Another possibility for the combined evaluation of rejection and fouling was proposed by Smolders at the workshop on characterization of UF membranes in Örenäs (see table 7) [66]. This approach suggests the measurement of rejection of four different types of substances, differing in molecular weight and hydrophilicity and thus exhibiting different degrees of rejection, fouling and concentration polarization.

6 Combination of Methods

It has been accepted nowadays that only by using various characterization methods, fundamental aspects of the membrane and the separation process itself can be understood. Especially anisotropic polymeric membranes have very intricate structures, which cannot be characterised by one technique. Although some techniques are compatable, and in principle render the same results, it is not always clear whether the measured parameters really are responsible for the actual membrane performance.

Table 7. *Possible solutes for combined rejection and fouling studies [66]*

MW	*amphipolar*	*unipolar*
low	surfactants	sugar derivatives low MW ethers
high	proteins	carbohydrates polyethers

6.1 Gas Adsorption-Desorption, Thermoporometry and the Gold Sol Method

The pore size distributions obtained for the γ-alumina membrane by means of gas adsorption-desorption and thermoporometry (figure 9 and 14 respectively), illustrate the compatibility of both methods for this sort of media. Pore sizes and pore size distributions found with both methods are similar and also the porosity values (pore volume) are not significantly different (45 %) [3, 38, 60, 61].

The pore size distributions of PPO membranes are given in figures 10 (gas adsorption-desorption) and 15 (thermoporometry) respectively. Also here, both techniques render the same very narrow size distribution, with the average pore size of about 2 nm.

Since PPO membranes are made by the immersion precipitation method, the skin is assumed to be the most dense part of the membrane which contains the smallest pores. When the pore volume determined by thermoporometry and gas adsorption-desorption is expressed as volume per unit area of top layer (instead of volume per gram of membrane), the skin thickness can be estimated when a pore model of the skin, i.e., a value for the porosity, is assumed. For instance, for PPO membranes a pore volume of $150*10^{-6}cm^3/cm^2$ is found which implies that, when the porosity is set at 100% (so irrealistically, there is *no* polymer present in the skin), the 'skin thickness' would be 1.5 μm. The skin thickness of PPO membranes determined with the

more direct technique: the gold sol method, appeared to be sharply defined, having a thickness of 0.2 μm and a pore size very much different from that in the macroporous supporting layer. This thickness does not agree with the smallest thickness that can be calculated from the pore volume (found with thermoporometry or gas adsorption-desorption). It has to be concluded that the pores detected by thermoporometry and gas adsorption-desorption cannot be present in the skin only, but a large part of the pore volume must be related to pores in the sublayer.

6.2 Permporometry

The size distributions of the active interconnected pores obtained for the different membranes are presented in figure 18 and 19. For the PPO membranes the number of pores was calculated using a skin thickness of 0.2 μm, as determined with the gold sol method.

The size distribution of the active pores of alumina membranes (fig. 19) again appears to be very narrow. The average radius agrees well with the values found with the other techniques, i.e., gas adsorption- desorption and thermoporometry. This means that the pores responsible for the performance of the membranes really have a size of about 2 nm. From the number of pores and their sizes, the porosity of the γ-alumina membrane is calculated to be ~1%, a value which is very low compared to the porosity obtained from, e.g., thermoporometry. One of the reasons for this deviation is the very high tortuosity value (τ ~13) of the alumina system which is due to the high aspect ratio of the γ-alumina particles [12]. Furthermore it can be calculated that the thick sublayer of the alumina membrane is responsible for 70 % of the resistance for diffusional transport of the total system. Since diffusion is the main transport mechanism in permporometry, the effective driving force across the γ-alumina layer is only 30 % of the total during permporometry measurements. When the corrections for the tortuosity (so τ =13 instead of the hypothetical τ =1) and the resistance of the sublayer are used, the calculated porosity is about 40% which agrees with the value found earlier [12].

The size distribution of the open pores in PPO membranes, given in figure 18is much broader than the pore size distributions determined with gas adsorption-desorption or thermoporometry (figure 10 and 15). The largest pore sizes appear to be ~15 nm, but also pores of a few nanometers are present. Also, PPO membranes exhibit a very low skin porosity; 0.5 % for PPO, which is a quite normal value for UF membranes [21].

The differences between the pore size distributions measured with permporometry and the ones obtained from thermoporometry and gas adsorption-desorption, can be explained by the pore structure of the membranes and the specific physical phenomena on which the characterization techniques are based. With the two latter techniques all the volume of the (meso)pores present in the whole membrane (skin and sublayer) is measured. Since the volume of the pores present in

the skin is very low, it is difficult to detect it with, e.g., thermoporometry. On the other hand, when a considerable number of mesopores is present in the sublayer, these will be measured. Since thermoporometry and gas adsorption-desorption cannot discriminate between pores in the skin and those in the sublayer, the interpretation of the results may be difficult. With permporometry the interconnected open pores present in the skin are detected directly, based on their relative importance for the transport through the membrane. As a consequence, even pores which are present in a very small number (~low pore volume) are detected, provided the gas transport through these pores is high enough to be measured.

The Prediction of the Pure Water Flux

From the characterization methods discussed in this paragraph permporometry and the gold sol method are the only techniques which yield characteristic parameters that are really related to the performance of an UF membrane. In order to check the applicability of these characteristics the 'theoretical' pure water flux ($J_{aq,th}$) of the membanes was calculated using the Poiseuille equation (8) and subsequently compared with the experimental fluxes [3].

$$J_{aq,th.} = \{ \pi n r^4 \Delta p \} / \{ 8 \mu \tau l \} \qquad (8)$$

n : number of pores ($1/m^2$)
r : pore radius (m)
μ : viscosity (kg/ms)
Δp : pressure gradient (Pa)
τ : tortuosity (-)
l : thickness of the active layer (m)

In these calculations the tortuosity factor was assumed to be 1, and for PPO and PSf membranes a skin thickness of 0.2 μm was used. The results of these calculations are summarized in table 8.

One can see that theoretical and experimental pure water fluxes for each type of membrane separately do agree quite well. Also the experimental and calculated pure water fluxes of the alumina membranes agree reasonably well, provided that the data are corrected for the resistance of the sublayer. This indicates that the characteristic parameters of the membranes found with permporometry *and* gold sol method are indeed relevant for the transport properties of the membranes.

Table 8. *Comparison of experimental and calculated pure water fluxes*

membrane	*water flux (l/m2 hbar)*	
	calculated	*experimental*
γ-alumina*)	2.0-2.5	2.8-3.0
PPO	13-46	15-80

*) *data corrected for the resistance of the supporting layer, see also text*

7 Models Describing the Porous Structure

The description of the relation between the pore structure and the observed physical phenomena can be considered as another key-problem in characterization. The first models, which mainly described the pore morphology, originated from the researchers of porous charcoal [9] and were adapted to be used for a wide range of porous media. In these approaches the porous structure is visualized as a network of channels of different size and also dead-end pores are present. Especially for catalysts, such models appear to describe effective diffusion processes quite succesfully [67]. This is partly due to the simple nature of the free molecular diffusion regime which is predominant inside these systems. In fact, the pores are only needed to increase the relative area per volume of catalyst.

The description of transport through (and not only in) porous media appeared to be more complicated, as Mason indicated in his 'Dusty Gas Theory' [68]. Mason pointed out that transport through and in porous media is the resultant of different interfering transport mechanisms (diffusive and convective flow). Only in few situations one transport regime prevails and a simple model can be applied. Because of the large variety of models describing different physical phenomena, we will focus on the approaches which are of importance for membrane systems. Already in 1934 Ferry tried to model the transport of small, non-interacting particles through a membrane [69]. In this model the only factor affecting the rejection is the steric hindrance which is, of course, a gross oversimplification. An important conclusion from Ferry's approach is that the separation performance of a membrane process, in which size exclusion is the only separation mechanism, has only limited 'resolution'. This means that the cut-off value is always somewhat diffuse (figure 20). Several extensions of Ferry's theory were introduced which mainly made corrections for the hydrodynamic drag forces on the solute moving inside the pore. An extensive review of similar transport mechanisms has been given by Deen [70].

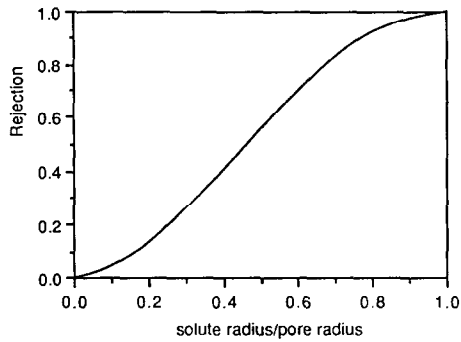

Figure 20. Rejection curve according to Ferry [69]. Rejection versus the ratio of solute size and cylindrical) pore radius.

Percolation Theory

Another 'class' of theories that receives more attention nowadays is the 'percolation approach'. In the percolation models the movement of a particle through a three dimensional network, imagined as a set of diffusion steps, is literally simulated [71, 72]. One of the reasons for the growing interest in this theory is the increased power of computers, which permits the simulation of complex systems, containing three or more permeating components [73]. The elegance of the simulations is that the interference between small and large particles, which together penetrate the porous medium, can be shown. Although the particles have no specific affinity towards each other or to the membrane, their transport through the pores is influenced by the fact that particles cannot 'travel' freely throughout the medium. Besides that, not each diffusive movement will be an effective step 'to the other side' of the membrane and the more the pores are interconnected, the more the particle can 'get lost' inside the system. The magnitude of the driving force will influence the transport through the network too, because it will change the path of the particle through the network. Altogether this means that at a low degree of interconnectivity, which might be expected for a medium that possesses a very low porosity (like UF membranes), percolation theory can be relatively simply applied.

Fractal Theory

Recently, the fractal nature of a porous medium was recognized. The term 'fractal' [73] refers to purely geometric properties of the objects and means that a structure is built of selfsimilar entities (figure 21). As the transport properties of porous media are determined by the structural geometry, the fractality will have its impact on the hydrodynamic behaviour of the system [74]. The fractal nature of porous media can be approached from three different ways: the pore space, the solid and the solid-pore interface. For characterization the first one appears to be the most interesting approach. A major advantage of fractal theories is the possibility to describe very complex systems, as porous media are, in a simple way. Although, until now, fractal geometry has only made conceptual progress in treating complex geometries, prospects for the future are interesting [75].

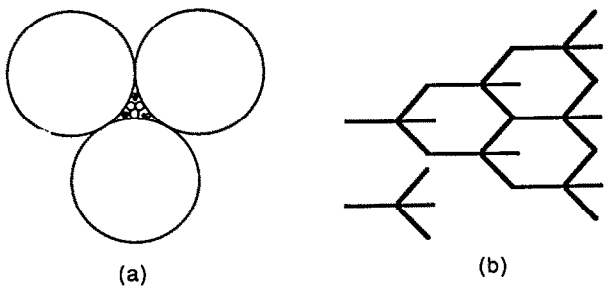

Figure 21. Model of two physical situations described by regular fractals, (a) the solid is fractal, (b) the pore structure is fractal [75].

For UF membranes it is not clear whether a fractal description of the pores can be used. Since the porosity of the top layer is very low, the pore structure itself can be hardly imagined as fractal. It might be possible that the solid exhibits fractal nature, for instance in the form of a 'nodular structure'. But as neither the structures of UF membranes nor that of the nodules have been revealed yet, even this problem is only hypothetical.

8 Conclusions

From the foregoing it is clear that, for a proper characterization of membranes, a number of conditions should be fulfilled. In the first place the structure of the membrane should be known in relation to the performance or physical parameters that have to be described. In membrane science one is primarily interested in characteristics which can describe the membrane performance, preferably for a wide range of applications. The elucidation of the relations between membrane structure and membrane performance require the use of different methods and since the prediction of performance is directly related to the distribution of the active pores and the thickness of the top layer, techniques should be focussed on the measurement of such active parameters.

9 Literature

1. Kesting, R.E. in ' Synthetic Polymer Membranes', McGraw Hill, New York, 1972
2. Gelman, C., Analytical Chemistry 37 (1965) 29A
3. Cuperus, F.P., Characterization of UF membranes, Thesis University of Twente, the Netherlands, 1990
4. Bechhold, H., Z. Phys. Chem. 60 (1907) 328
5. Zsigmondi, A., Z. Anorg. Chem. 71 (1911) 356
6. Trägård, G. in 'Characterization of Ultrafiltration Membranes', G. Trägård (ed.), p.9, Lund University, Lund, Sweden, 1987
7. Everett, D.H. in 'Characterization of Porous Solids', K.K.Unger, J. Rouquerol, K.S.W. Sing and H.Kral (eds.), p. 1, Elsevier, Amsterdam, 1988
8. ESMST Report on Terminology for Pressure Driven Membrane Operations 1986, Desalination 68 (1988) 77
9. Gregg, S.J. and Sing, K.S.W. in 'Adsorption, Surface Area and Porosity', 1st edition, 1967; 2nd edition, 1982, Academic Press, London
10. IUPAC Reporting Physisorption Data, Pure Appl. Chem. 57 (1985) 603
11. Te Hennepe, H.J.C., Zeolite Filled Polymeric Membranes, Thesis University of Twente, the Netherlands, 1988
12. a.Keizer, K.K., Burgggraaf, A.J. in 'Porous Ceramic Materials in Membrane Applications

in 'Science of Ceramics 14', B. Taylor (ed.), p.83, Institute of Ceramics, Shelton UK, 1988; b.Uhlhorn R.J.R., Ceramic Membranes for Gas Separation, Thesis University of Twente, the Netherlands, 1990.

13. Nijhuis, H.H., Removal of Trace Organics by Pervaporation, Thesis University of Twente, the Netherlands, 1990
14. van den Berg, G.B., Concentration Polarization, Thesis University of Twente, the Netherlands, 1988
15. Klein, E., Feldhof, P., Turnham, T., J. Membrane Sci. 15 (1983) 245
16. Lakshminarayanaiah, N., Chem. Reviews 65 (1965) 491
17. Michaels, A.S., Sep.Sci. and Techn. 15 (1980) 1305
18. Mason, E.A., Wendt, R.P., Bresler, E.H., J. MembraneSci. 6 (1980) 283
19. Wendt, R.P., Klein, E., J. MembraneSci. 17 (1984) 161
20. Michaels, A.S., Preprints ICOM 1987, p.17, June 8-12 1987, Tokyo, invited lecture 5
21. Fane, A.G., Fell, C.J.D. in 'Characterization of UF Membranes', G. Trägård (ed.), p.39, Lund University, Lund Sweden, 1987
22. Gekas, V., Zhang, W., Process Biochemistry 29 (1989) 159
23. Matson, S., US Patent, nr. 4,800,162, Januari 24, 1989
24. Oldani, M., Schock, G., J. Membrane Sci. 43 (1989) 243
25. Franken, A.C.M., Nolten, J.A.M., Mulder, M.H.V., Bargeman, D., Smolders, C.A., J. Membrane Sci. 33 (1987) 315
26. Banerji, B.K., Colloid and Polymer Sci. 259 (1981) 391
27. Keurentjes, J., van't Riet, K., J. Membrane Sci. 117 (1989) 333
28. Absolon, J., J. Colloid Interface Science 117 (1987) 550
29. Adamson, A.W. in 'Physical Chemistry of Surfaces', 2nd edition, Chapter vii, Wiley, New York, 1967
30. Cook, M.A. in 'Hydrophobic Surfaces' F.M. Fowkes (ed.), p. 206, Academic Press, New York, 1969
31. Martinez, L., Gigosos, M.A., Hernandez, A., Tejarina, F., J. Membrane Sci. 35 (1987) 1
32. Nyström M., Lindström, M., Matthiasson, E., J. Membrane Sci. 36 (1989) 297
33. McDonogh, P.M., Fell, C.J.D., Fane, A.G., J. Membrane Sci. 21 (1984) 1285
34. Lecloux, A.J., Pirard, J.P., J. Colloid Interface Sci. 70 (1979) 265 and in 'Characterization of Porous Solids', K.K.Unger, J. Rouquerol, K.S.W. Sing and H.Kral (eds.), p. 233, Elsevier, Amsterdam, 1988
35. Eyraud, C., Betemps, M., Quinson, J.F., Bull. Soc. Chim. France 9-10 (1984) I-238
36. Smolders, C.A., Vugteveen, E., Polym. Mater. Sci. Eng. 50 (1984) 177
37. Zeman, L., Tkacik, G. in ' Material Science of Polymeric Membranes', D.R. Loyd (ed.), p.339, ACS Symposium Series no. 269, Am. Chem. Soc.,Washington, DC, 1984
38. Brun, M., Quinson, J.F., Spitz, R., Bartholin, M., Makromol. Chem. 183 (1982) 1523
39. Lange, R.H., Blödorn, J., Das Elektronen Microskop: TEM & SEM, Thieme Verlag, Stuttgart, 1981

40. Vivier, H., Pons, M., Portala, F., J. Membrane Sci. 46 (1989) 81
41. Roesink, H.D.W., Microfiltration, Thesis University of Twente, the Netherlands, 1989
42. Fane, A.G., Fell, C.D.J., Waters, A.G., J. Membrane Sci. 9 (1981) 245
43. Merin, U., Cheryan, M., J. Appl. Pol. Sci. 25 (1980) 2139
44. Von Preusser, H.J., Kolloid-Z.Z. Polym. 250 (1972) 133
45. Fane, A.G., Fell, C.J.D., Desalination, 62 (1987) 117
46. Baker, R.W., Erich, F.R., Strathmann, H., J. Phys. Chem. 76 (1972) 238
47. Capanelli, G., Vigo, F., Munari, S., J. Membrane Sci. 15 (1983) 289
48. Hanemaaijer, J.H. Robbertson, T., van den Boomgaard, Th., Olieman, C., Both, P., Schmidt, D.G., Desalination 68 (1988) 93
49. Sarbolouki, M.N., J. Appl. Pol. Sci. 29 (1984) 743
50. Cuperus, F.P., Bargeman, D., Smolders, C.A. J. Colloid Interface Sci, 135 (1990) 486
51. Altena, F.W., Knoef, H.A.M., Heskamp, H., Bargeman, D., Smolders, C.A., J.MembraneSci. 12 (1983) 313
52. a. Erbe, F., Kolloid Z. 59 (1932) 195; b. Bechhold, H., Schlesinger, M., Silbereisen, K., Kolloid Z. 55 (1931) 172
53. Meltzer, T.H., Bull. Par. Drug Ass. 25 (1971) 165
54. Franken, A.C.M., Membrane Distillation, Thesis, University of Twente, the Netherlands, 1988
55. Grabar, P., Nikitine, S., J. Chim. Phys. 33 (1936) 50
56. Munari, S., Bottino, A., Moretti, P., Capanelli, G., Becchi, I., J. Membrane Sci. 41 (1989) 68
57. Kujawski, W., Adamczak, P.A., Narebska, A., Sep. Sci. and Techn. 24 (1989) 495
58. Conner, Wm.C., Lane, A.M., J. Catalysis 89 (1984) 217
59. Liabastre, A.A., Orr, C., J. Colloid Interface Sci. 64 (1978) 1
60. Brun, M., Lallemand, A., Quinson, J.F. and Eyraud, Ch., Thermochim. Acta 21 (1977) 59
61. Eyraud, Ch., Quinson, J.F. and Brun, M. in 'Characterization of Porous Solids', K.K. Unger, J. Rouquerol, K.S.W. Sing and H.Kral (eds.), p. 295, Elsevier, Amsterdam, 1988
62. Eyraud, Ch., Betemps, M. and Quinson, J.F., Bull. Soc. Chim. France 9-10 (1984) I-238
63. a. Mey-Marom, A., Katz, M.J., J. Membrane Sci. 27 (1986) 119; b. Katz, M., Baruch, G., Desalination 58 (1986) 199
64. Jones, B.R., Wade, W.H. in 'Hydrophobic Surface', F.M. Fowkes (ed.), p.206, Academic Press, New York, 1969.
65. a. Bohrer, M.P., I & EC fund. 22 (1983) 72; b. Bohrer, M.P., Patterson, G.D., Carol, P.J., Macromol. 18 (1985) 2531
66. Gekas, V. in 'Characterization of UF Membranes', G. Trägård (ed.), p.245, Lund University, Lund Sweden, 1987
67. Satterfield, C.N., Cadle, P.J., I & EC fund. 7 (1968) 202
68. Mason, E.A., Malinouskas, A.P. in 'Gas Transport in Porous Media: the Dusty Gas Model', Amsterdam, Elsevier, 1983

69. Ferry, Chem. Rev. 18 (1936) 373
70. Deen, W.M., AIChE Journal 33 (1987) 409
71. Shante, V.K., Kirkpatrick, S., Advances in Physics 20 (1971) 325
72. Kirkpatrick, S., Advances in Modern Physics 45 (1973) 574
73. Gyer, R. A., Phys. Rev. 37 (1988) 5713
74. Farin, D., Avnir, D. in 'Characterization of Porous Solids', K.K.Unger, J. Rouquerol, K.S.W. Sing and H.Kral (eds.), p. 421, Elsevier, Amsterdam, 1988
75. Adler, P.M. in 'Characterization of Porous Solids', K.K.Unger, J. Rouquerol, K.S.W. Sing and H.Kral (eds.), p. 433, Elsevier, Amsterdam, 1988